HHS Public Access

Author manuscript

Exp Neurol. Author manuscript; available in PMC 2024 March 01.

Published in final edited form as:

Exp Neurol. 2023 March ; 361: 114303. doi:10.1016/j.expneurol.2022.114303.

Plateau potentials contribute to myotonia in mouse models of myotonia congenital

Xueyong Wang[1], **Chris Dupont**[1], **Delaney Grant**[1], **Andrew A. Voss**[2], **Mark M. Rich**[1]

[1]Department of Neuroscience, Cell Biology and Physiology, Wright State University, Dayton, OH, 45435.

[2]Department of Biology, Wright State University, Dayton, OH, 45435.

Abstract

It has long been accepted that myotonia (muscle stiffness) in patients with muscle channelopathies is due to myotonic discharges (involuntary firing of action potentials). In a previous study, we identified a novel phenomenon in myotonic muscle: development of plateau potentials, transient depolarizations to near −35 mV lasting for seconds to minutes. In the current study we examined whether plateau potentials contribute to myotonia. A recessive genetic model (ClC^{adr} mice) with complete loss of muscle chloride channel (ClC-1) function was used to model severe myotonia congenita with complete loss of ClC-1 function and a pharmacologic model using anthracene-9-carboxylic acid (9AC) was used to model milder myotonia congenita with incomplete loss of ClC-1 function. Simultaneous measurements of action potentials and myoplasmic Ca^{2+} from individual muscle fibers were compared to recordings of whole muscle force generation. In ClC^{adr} muscle both myotonia and plateau potentials lasted 10s of seconds to minutes. During plateau potentials lasting 1–2 minutes, there was a gradual transition from high to low intracellular Ca^{2+}, suggesting a transition in individual fibers from myotonia to flaccid paralysis in severe myotonia congenita. In 9AC-treated muscles, both myotonia and plateau potentials lasted only a few seconds and Ca^{2+} remained elevated during the plateau potentials, suggesting plateau potentials contribute to myotonia without causing weakness. We propose, that in myotonic muscle, there is a novel state in which there is contraction in the absence of action potentials. This discovery provides a mechanism to explain reports of patients with myotonia who suffer from electrically silent muscle contraction lasting minutes.

Graphical Abstract

Please address all correspondence to: Mark Rich, mark.rich@wright.edu.

Declarations of interest: none

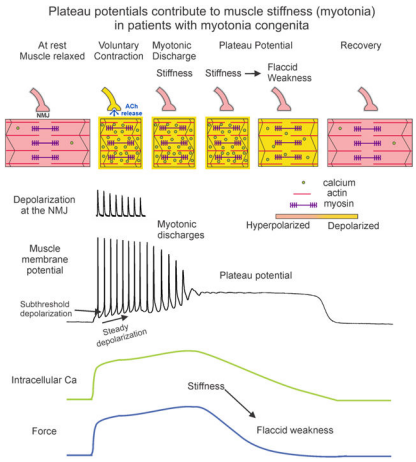

Keywords

myotonia; muscle; excitability; action potential; stiffness; weakness

Introduction:

Muscle dysfunction in myotonia congenita results from loss-of-function mutations in the muscle chloride channel (ClC-1) (Koch, et al., 1992; Steinmeyer, et al., 1991). There are two forms of myotonia congenita, a recessively inherited form (Becker's disease) and a dominantly inherited form (Thomsen's disease). In both forms there is a loss of ClC-1 channel function (Cannon, 2015; Lehmann-Horn, et al., 2008; Trivedi, et al., 2014) and a prominent symptom is myotonia (muscle stiffness), which is thought to be due to myotonic discharges (continued firing of action potentials following termination of voluntary contraction). However, there have been reports of patients with myotonia who suffered from electrically silent muscle contraction (Sanders, 1976; Stohr, et al., 1975). In these patients, myotonic discharges cannot be the only mechanism contributing to myotonia.

Many patients with Becker's disease suffer from transient weakness in addition to myotonia (Lehmann-Horn, et al., 2008; Ricker, et al., 1978; Trivedi, et al., 2014). In a recent study we discovered a mechanism that may be responsible for transient weakness: development of plateau potentials. Plateau potentials consist of depolarization of the membrane potential to near −35 mV, which can last seconds to minutes (Myers, et al., 2021). Depolarization during plateau potentials causes inactivation of Na^+ channels necessary for generation of action potentials such that muscle becomes electrically inexcitable. Without the ability to generate action potentials muscle fibers are paralyzed during plateau potentials. Prevention of plateau potentials eliminated transient weakness in a mouse model of Becker's disease.

Depolarization to −35 mV may be sufficient to trigger excitation contraction coupling: the process by which charge movement of Cav1.1 channels in t-tubules triggers opening of ryanodine receptors and release of Ca^{2+} from the sarcoplasmic reticulum (Braubach, et al., 2014; Wang, et al., 2022; Wang, et al., 1999). If plateau potentials trigger excitation contraction coupling, they could cause persistent muscle contraction (myotonia)

in electrically silent muscle. To better understand the contribution of plateau potentials to muscle dysfunction in a severe and a milder mouse model of myotonia congenita, we performed force recordings as well as simultaneous intracellular recording and Ca^{2+} imaging in both a recessive genetic model with complete loss of muscle ClC-1 channel function as well as a pharmacologic model with incomplete loss of ClC-1 channel function. Intracellular Ca^{2+} was elevated during the early phase of plateau potentials in both models, suggesting plateau potentials contribute to myotonia. During prolonged plateau potentials, which only occurred in the severe model, Ca^{2+} fell to low levels such that flaccid paralysis would be expected. We conclude plateau potentials contribute to myotonia in both mildly and severely affected patients. In severely affected patients, plateau potentials also cause transient weakness.

Methods:

Mice

All animal procedures were performed in accordance with the policies of the Animal Care and Use Committee of Wright State University and were conducted in accordance with the United States Public Health Service's Policy on Humane Care and Use of Laboratory Animals. The genetic mouse model of myotonia congenita used was *Clcn1*$^{adr\text{-}mto}$/J (ClC^{adr}) mice, which have a homozygous null mutation in the *Clcn1* gene (Jackson Labs cat #000939) and were used to model Becker's disease. In the pharmacologic model, muscle was treated with 100 μM 9-anthracenecarboxylic acid (9-AC) ex vivo, which causes a greater than 90% reduction in Cl^- conductance (Palade and Barchi, 1977).

Mice expressing GCAMP6f (Chen, et al., 2013) in skeletal muscle were generated by crossing floxed GCAMP6f mice (Jackson Labs, B6J.Cg-*Gt(ROSA)26Sortm95.1(CAG-GCaMP6f)Hze*/MwarJ, cat #028865) with mice expressing parvalbumin promoter driven Cre (Jackson Labs, B6.129P2-Pvalbtm1(cre)Arbr/J, cat# 030218). These mice were either treated with 9AC or crossed with ClC^{adr} mice for two generations to obtain mice expressing GCAMP6f, which were also homozygous for knockout of ClC-1 chloride channels.

Genotyping of ClC^{adr} mice was performed as previously described to select heterozygous mice for breeding (Dupont, et al., 2019). Otherwise, homozygous myotonic mice were identified by appearance and behavior as previously described (Novak, et al., 2015). Both male and female mice were used from 2 months to 6 months of age. As mice with myotonia have difficulty climbing to reach food, symptomatic mice were supplied with moistened chow paste (Irradiated Rodent Diet; Harlan Teklad 2918) on the floor of the cage.

Mice were sacrificed using CO_2 inhalation followed by cervical dislocation.

Force recording

All experiments were performed on EDL muscles at 21–23°C within 4 hours of sacrifice. The *extensor digitorum longus* (EDL) muscle was dissected, placed in a custom recording chamber and perfused with Ringer solution containing (in mM): 118 NaCl, 3.5 KCl, 1.5 $CaCl_2$, 0.7 $MgSO_4$, 26.2 $NaHCO_3$, 1.7 NaH_2PO_4, with 5.5 glucose and maintained at pH 7.3–7.4 by aeration with 95% O_2 and 5% CO_2. The proximal tendon was tied with a 6–0

caliber silk suture to a bar and the distal tendon was tied to a hook and attached to a force transducer (Aurora Scientific). The EDL was stimulated with two platinum electrodes placed parallel to the muscle in the bath. Optimal length was determined by adjusting the tension of the muscle until maximal twitch force was achieved. To induce myotonia, the EDL was stimulated with 40 pulses of 1 ms duration delivered at 100 Hz. Force was recorded using a CED 1401 A to D board using Spike2 software (Cambridge Electronic Design Limited). No filtering was applied to the signal.

Intracellular recording

The same solution used for force recording was perfused into the bath. For experiments in which Ca^{2+} imaging and intracellular recording were performed, contraction was prevented by loading muscles with 50μM BTS (N-benzyl-p-toluenesulfonamide, Tokyo Chemical Industry, Tokyo, Japan, catalogue #B3082) dissolved in DMSO for 45 minutes prior to recording. Muscle fibers were impaled with 2 sharp microelectrodes filled with 3 M KCl solution containing 1 mM sulforhodamine 101 (Sigma-Aldrich, Catalogue #S7635) to allow for visualization. Electrode resistances were between 10 and 30 MΩ, and capacitance compensation was optimized prior to recording. Action potentials were evoked by a 0.2 ms injection of current ranging from 100 to 1000 nA. Fibers with resting potentials more depolarized than −74 mV were discarded. Sampling frequency was 50 kHz with a 5 kHz low pass filter.

Imaging of ΔF/F

Muscle expressing GCAMP6f was imaged with a 40x objective without staining (Leica I3 cube, band pass 450–490, long pass 515) as previously described (Wang, et al., 2022). Imaging was synchronized with triggering of action potentials using a Master-8 pulse generator (A.M.P.I., Jerusalem). Frames were acquired at 30 frames per second with a sCMOS camera (CS2100M-USB) using ThorCam software (Thorlab Inc. NJ). Images were analyzed using Image J (NIH) using the average of several regions of interest along the length of the stimulated fiber. Background was subtracted using the average of several regions of interest on a neighboring fiber, which was not stimulated.

To confirm that the sampling rate of 30 Hz was not missing an early peak in Ca^{2+} signal, we imaged a subset of fibers using a photomultiplier tube (Thorlab Inc. NJ) with a sampling rate of 5 kHz. The fluorescence signal 33 ms after triggering the AP averaged 96.2 ± 0.8% of the peak signal, measured using the photomultiplier tube (which occurred at 44.3 ± 3.2 ms (n = 9 muscles)). These data suggest the sampling frequency of 30 Hz introduced a slight underestimation of the peak ΔF/F.

To compare ΔF/F between fibers, the signal for each fiber was normalized to the peak signal in that fiber. The peak signal usually occurred during a myotonic discharge, but could also occur during the early phase of a plateau potential. To determine the ΔF/F sufficient to trigger contraction, the peak ΔF/F following a single action potential was normalized to the maximal signal during a myotonic discharge/plateau potential for that fiber. Only fibers with Ca^{2+} signal measurement following both a single action potential and a myotonic discharge/plateau potential were analyzed.

Statistics

For comparisons of whole muscle force or Ca^{2+}, a student's t-test was performed. For comparisons of data collected from individual fibers, nested analysis of variance was performed with n as the number of muscles studied. All data is presented as mean ± SD. $p < 0.05$ was considered to be significant.

Results

Two mouse models of myotonia congenita were studied. A recessive genetic model (ClC^{adr} mice) with complete loss of muscle chloride channel function modeled severe myotonia congenita (Steinmeyer, et al., 1991). A pharmacologic model using 100 μM 9-anthracenecarboxylic acid (9AC) to block more than 90% of muscle chloride channels (Palade and Barchi, 1977) modeled milder disease. Tetanic force recordings were performed on whole EDL muscles and myotonia was triggered by stimulation at 100 Hz for 40 pulses (Fig. 1). The duration of myotonia (time for myotonia to decrease by 95% from its peak) differed between the two models and averaged 27.4 ± 19.3 s in ClC^{adr} muscles (n = 10 muscles) versus 9.0 ± 5.0 s in 9AC-treated muscles (n = 11 muscles, $p < 0.001$, Fig 1). For reference, tetanic force in noncarrier wild type (WT) muscle decreased by 95% of peak tetanic force in an average of 0.2 ± 0.1 s (n = 4 muscles).

To ascertain the contribution of plateau potentials to myotonia, it is necessary to simultaneously measure membrane potential and either force or a surrogate for force. Since intracellular recording cannot be performed while measuring force, we used Ca^{2+} imaging to assess whether changes in membrane potential were associated with contraction. Ca^{2+} was imaged in muscles expressing GCAMP6f, a Ca^{2+} indicator with a Kd near 600 nM in cardiomyocytes such that it can detect changes in Ca^{2+} ranging from 100 nM to 5 uM (Shang, et al., 2014; Wang, et al., 2022).

To image Ca^{2+} in the recessive genetic model of myotonia congenita, mice expressing GCAMP6f were crossed for two generations with ClC^{adr} mice to generate homozygous ClC^{adr} mice that expressed GCAMP6f. To perform Ca^{2+} imaging in the 9AC model of myotonia congenita, control muscle expressing GCAMP6f was treated with 9AC. The 95% decay time of whole muscle ΔF/F following 0.4s of 100 Hz stimulation in wild type muscle was 0.6 ± 0.1 s (n = 10 muscles). The slow decay of signal in wild type muscle suggests a limitation of GCAMP6f is that its kinetics are too slow for accurate analysis of the kinetics of Ca^{2+} handling in normal muscle. The 95% decay time of ΔF/F ClC^{adr} mice, averaged 45.9 ± 7.4 s in (n = 10 muscles) versus 6.1 ± 4.0 s in 9AC treated muscle (n = 10 muscles, $p < 0.001$, Fig 1). These data demonstrate that the longer duration of myotonia in the ClC^{adr} model is paralleled by prolonged elevation of intracellular Ca^{2+}.

To simultaneously measure Ca^{2+} while recording membrane potential, the brightness of several regions of interest imaged near the electrodes was averaged during recordings from individual fibers. In wild type muscle expressing CGAMP6f ($WT_{GCAMP6f}$) a robust Ca^{2+} signal was generated by a single action potential (Fig 2A and B). Stimulation with 0.2 ms injections of current into the impaled fiber at 100 Hz in $WT_{GCAMP6f}$ fibers caused elevation of ΔF/F throughout the period of stimulation with a decay to near baseline 0.5

s after termination of stimulation (Fig 2C). In 9AC treated muscle ($9AC_{GCAMP6f}$), there was continued firing of action potentials following termination of stimulation, which was accompanied by continued elevation of the Ca^{2+} signal (Fig 2D).

Intracellular membrane potential and Ca^{2+} were simultaneously measured in 20 fibers from 10 ClC^{adr} mice expressing GCAMP6f ($ClC^{adr}_{GCAMP6f}$). In all fibers there were two phases of pathologic depolarization following termination of 100 Hz stimulation. The first phase consisted of myotonic discharges, which transitioned into the second phase: development of plateau potentials, prolonged depolarization to near −35 mV (Fig 3). ΔF/F rose during myotonic discharges, and initially remained elevated during plateau potentials, followed by a slow decay. The horizontal dashed line in Fig. 3 indicates the ΔF/F in response to a single action potential (twitch). We assumed that myotonia (stiffness) was present at least as long as intracellular Ca^{2+} remained elevated above the level during a twitch. In the examples shown in Fig 3 this was between 20 and 30s for each fiber. Often there were oscillations in the membrane potential prior to termination of the plateau potential, which triggered oscillations in ΔF/F. These data suggest there is ongoing Ca^{2+} release from intracellular stores or ongoing entry of extracellular Ca^{2+} during plateau potentials (Fig 3). Upon termination of plateau potentials, there was a rapid return of ΔF/F to baseline.

The time course and relative contribution of myotonic discharges and plateau potentials to prolonged elevation of ΔF/F in $ClC^{adr}_{GCAMP6f}$ fibers were estimated as follows. In each fiber, the elevation of ΔF/F above baseline at each time point was attributed to myotonic discharges or plateau potentials as shown in Fig 4A. The data for all 20 fibers was pooled and the proportion of the elevation of ΔF/F, which could be ascribed to myotonic discharges or plateau potentials was plotted versus time (Fig 4B). Almost all of the initial elevation of ΔF/F was due to myotonic discharges, but the proportion dropped as fibers transitioned into plateau potentials by 10 s. The contribution of plateau potentials to elevation of ΔF/F peaked near 15 s. There was a slow decrease over the next minute in ΔF/F due both to termination of plateau potentials and a drop in ΔF/F during plateau potentials. These data are consistent with the possibility that the early phase of myotonia is primarily due to myotonic discharges, but the late phase is due to plateau potentials.

In $9AC_{GCAMP6f}$ muscle, plateau potentials ranged from 1 to 5 s in duration (Fig 5A). These data agree with our previous finding that plateau potentials in the ClC^{adr} mouse model tend to be longer than plateau potentials triggered by application of 9AC (Myers, et al., 2021). Because plateau potentials were brief following 9AC treatment, ΔF/F remained above the average value for ΔF/F following single action potentials for the majority of the duration of plateau potentials, suggesting fibers contract for the duration of plateau potentials (Fig 5A). Of note, the value for ΔF/F following a single action potential compared to 100 Hz stimulation significantly differed between $ClC^{adr}_{GCAMP6f}$ and $9AC_{GCAMP6f}$ fibers (0.22 ± 0.07 vs 0.37 ± 0.08, $p < 0.001$, n = 18 fibers from 9 mice for $ClC^{adr}_{GCAMP6f}$ and 372 fibers from 14 mice for $9AC_{GCAMP6f}$).

The percentage of fibers developing plateau potentials averaged 32%, but varied widely between experiments (Fig 5B). When the elevation of ΔF/F due to myotonic discharges versus plateau potentials was plotted, plateau potentials played little to no role in the early

phase of elevation of ΔF/F, and were never a major contributor to elevation of ΔF/F. This was because only a minority of fibers developed plateau potentials. Overall, these data suggest that while plateau potentials can develop, they are a minor contributor to myotonia in mild myotonia congenita. However, in the subset of muscles with a high percentage of fibers with plateau potentials, they may contribute.

Discussion:

Using two mouse models of myotonia congenita, we describe a novel state of myotonic muscle in which muscle is electrically inexcitable, but contracting due to elevation of intracellular Ca^{2+} caused by steady depolarization. Prior to this study, the only mechanism that had been identified as underlying myotonia (stiffness) was myotonic discharges (involuntary action potentials) (Adrian and Bryant, 1974; Cannon, 2015; Matthews and Hanna, 2014; Trivedi, et al., 2014). Our data suggest a second contributor to myotonia is development of plateau potentials, depolarizations to near −35 mV, which last seconds to minutes. During prolonged plateau potentials there is a gradual drop in intracellular Ca^{2+} suggesting a slow transition from myotonia to flaccid paralysis in individual fibers.

The contribution of plateau potentials to muscle dysfunction in myotonia congenita

There have been reports of patients with myotonia who suffered from electrically silent muscle contractions lasting two to three minutes after exertion (Sanders, 1976; Stohr, et al., 1975). In those reports, the mechanism underlying electrically silent contraction was proposed to be a metabolic defect of muscle. Our findings that plateau potentials can last minutes and can sustain elevation of intracellular Ca^{2+} for minutes, suggest the mechanism is development of plateau potentials.

We previously reported plateau potentials are responsible for transient weakness in the ClC^{adr} mouse model of severe recessive myotonia congenita (Becker's disease, (Myers, et al., 2021)). Patients with milder myotonia congenita due to incomplete loss of muscle Cl current do not have transient weakness (Lossin and George, 2008; Trivedi, et al., 2014), but in the 9AC model of milder myotonia congenita, some fibers develop plateau potentials (Myers, et al., 2021). If plateau potentials always cause transient weakness, one would expect transient weakness to also be present in mild myotonia. Our current study suggests plateau potentials do not always cause transient weakness. Instead, during the first few seconds of plateau potentials, they contribute to myotonia because intracellular Ca^{2+} remains elevated. Only when plateau potentials are prolonged and intracellular Ca^{2+} drops, does transient weakness develop.

While our study suggests plateau potentials contribute to myotonia, there are two factors that make it difficult to quantitate the contribution. One is uncertainty about the percentage of fibers that develop plateau potentials. In a previous study, we found a higher percentage of fibers developed plateau potentials following treatment with 9AC (Myers, et al., 2021). In the current study, a higher percentage of fibers developed plateau potentials in ClC^{adr} mice. The variability in data following 9AC treatment is likely due to variability of block of ClC-1 channels. We have observed the duration of myotonic discharges and the percentage of fibers with plateau potentials increases as time spent recording in the presence of 9AC

increases. The higher percentage of fibers with plateau potentials from ClC^{adr} mice in the current study may be due to more careful handling of the muscle during dissection. Stretch of muscle during dissection triggers myotonia in ClC^{adr} muscle, which results in warm-up prior to recording, and decreases the percentage of fibers that develop plateau potentials.

A second reason for difficulty quantitating the contribution of plateau potentials to myotonia in vivo is that there were several limitations to our study. We did not perform intracellular recording while measuring muscle force. This is because contraction of impaled fibers causes membrane damage and loss of resting potential. Instead, we used non-ratiometric Ca^{2+} imaging of individual fibers during myotonia using a dye with slow kinetics as a surrogate for force. Limitations of the dye make it difficult to estimate force generated based on the Ca^{2+} signal. Furthermore, there is a non-linear relationship between intracellular Ca^{2+} and force (Lamb and Stephenson, 2018; Zot and Potter, 1987). Finally, our studies were performed at room temperature rather than at 37°C.

Despite limitations, our data suggest that in patients with prolonged myotonia, plateau potentials are an important contributor. Myotonic discharges rarely lasted more than 10 s, whereas plateau potentials could last minutes. In a subset of muscles, myotonia lasted much longer than 10 s. In those muscles it seems highly likely that the mechanism underlying prolonged myotonia is development of plateau potentials.

Part of the efficacy of Na^+ channel blockers in treating myotonia may derive from prevention of plateau potentials. Mexiletine is the first line choice of therapy for myotonia congenita and it is effective in lessening the transient weakness that is likely due to plateau potentials (Lo Monaco, et al., 2015; Statland, et al., 2012). The Na^+ channel blocker ranolazine eliminated plateau potentials at doses that did not fully eliminate myotonic discharges (Myers, et al., 2021). This suggests it may be easier to prevent plateau potentials than it is to eliminate myotonic discharges. If this holds true for other Na^+ channel blockers, this would suggest patients in which plateau potentials are an important contributor to muscle dysfunction may respond better to therapy with Na^+ channel blockers.

The sequence of events triggered by voluntary contraction of muscle in myotonia congenita

Combining current findings with our previous studies (Dupont, et al., 2020; Hawash, et al., 2017; Metzger, et al., 2020; Myers, et al., 2021) leads to the proposal that voluntary contraction initiates the sequence of events in myotonic muscle depicted in Fig 6. During voluntary movement, firing of muscle action potentials is triggered by depolarization at the neuromuscular junction. When voluntary contraction ceases, action potentials continue in myotonic muscle due to combination of steady and subthreshold depolarizations (Metzger, et al., 2020). Steady depolarization is likely due to build-up of K^+ in t-tubules (Adrian and Bryant, 1974; Adrian and Marshall, 1976; Fraser, et al., 2011; Wallinga, et al., 1999) and activation of TRPV4 channels by stretch of muscle membrane during contraction (Dupont, et al., 2020). The subthreshold depolarization responsible for reaching action potential threshold is due to a small, non-inactivating Na^+ current (Na^+ persistent current or NaP) (Hawash, et al., 2017). In normal muscle, ClC-1 Cl^- channels account for 70%−80% of resting muscle membrane conductance (Adrian and Bryant, 1974; Palade and Barchi, 1977),

and prevent NaP, K^+ build-up and activation of TRPV4 from depolarizing muscle enough to trigger myotonic discharges. In myotonia congenita, loss of function mutations in the ClC-1 channel reduce Cl^- conductance (Koch, et al., 1992; Steinmeyer, et al., 1991), such that the contributors to depolarization are sufficient to trigger myotonic discharges.

Once a myotonic discharge is triggered, it can either end with repolarization and recovery of normal excitability or with transition to a plateau potential (Myers, et al., 2021) (Fig 6). The transition to plateau potentials is due, at least in part, to overactivation of NaP, which transitions from activating intermittently during the approach to action potential threshold, to being on continually and causing steady depolarization (Myers, et al., 2021). Throughout plateau potentials muscle is inexcitable and thus unable to participate in voluntary movement. During the early phase of plateau potentials, muscle is contracting due to elevation of intracellular Ca^{2+}. This contraction is similar to the seconds-long contraction of muscle triggered by perfusion of solution with elevated extracellular K, which depolarizes fibers enough to directly trigger Ca^{2+} release from the SR and muscle contraction in the absence of action potentials (Chua and Dulhunty, 1988). During prolonged plateau potentials, there is a gradual reduction in intracellular Ca^{2+}. This may be due to at least three factors. The first is a gradual repolarization, which occurs during plateau potentials (Myers, et al., 2021). The second is inactivation of Ca^{2+} release from the sarcoplasmic reticulum (Schneider and Simon, 1988; Simon, et al., 1991). The third is depletion of sarcoplasmic reticulum Ca^{2+} (Robin and Allard, 2013). Studies of skinned muscle fibers have shown that over a 10-fold range of concentration, intracellular Ca^{2+} correlates with force generation (Lamb and Stephenson, 2018; Zot and Potter, 1987). Thus as intracellular Ca^{2+} decreases during plateau potentials, there is reduction of force generation in individual fibers such that fibers gradually transition from being stiff and paralyzed to flaccid and paralyzed. Finally, following termination of plateau potentials and repolarization of the membrane potential, there is recovery of excitability due to recovery from inactivation of the Na^+ channels responsible for action potentials. As the duration of myotonic discharges and plateau potentials varies widely between fibers, different fibers within a myotonic muscle will be in different states at the same time.

Conclusion

A novel state of myotonic muscle is described in which skeletal muscle is electrically inexcitable, but contracting due to depolarization to near −35 mV during plateau potentials. Prolonged plateau potentials in mice with severe myotonia congenita contribute sequentially to myotonia and transient weakness. Brief plateau potentials in a milder mouse model of myotonia congenita contribute primarily to myotonia.

Acknowledgements:

This work was supported by NIH grant AR074985 (M.M.R.) and MDA grant 602459 (https://doi.org/10.55762/pc.gr.84562, M.M.R.).

References

Adrian RH, and Bryant SH, 1974. On the repetitive discharge in myotonic muscle fibres. J Physiol 240, 505–515. [PubMed: 4420758]

Adrian RH, and Marshall MW, 1976. Action potentials reconstructed in normal and myotonic muscle fibres. J Physiol 258, 125–143. [PubMed: 940049]

Braubach P, Orynbayev M, Andronache Z, Hering T, Landwehrmeyer GB, Lindenberg KS, and Melzer W, 2014. Altered Ca(2+) signaling in skeletal muscle fibers of the R6/2 mouse, a model of Huntington's disease. J Gen Physiol 144, 393–413. [PubMed: 25348412]

Cannon SC, 2015. Channelopathies of skeletal muscle excitability. Compr Physiol 5, 761–790. [PubMed: 25880512]

Chen TW, Wardill TJ, Sun Y, Pulver SR, Renninger SL, Baohan A, Schreiter ER, Kerr RA, Orger MB, Jayaraman V, Looger LL, Svoboda K, and Kim DS, 2013. Ultrasensitive fluorescent proteins for imaging neuronal activity. Nature 499, 295–300. [PubMed: 23868258]

Chua M, and Dulhunty AF, 1988. Inactivation of excitation-contraction coupling in rat extensor digitorum longus and soleus muscles. J Gen Physiol 91, 737–757. [PubMed: 3418320]

Dupont C, Denman KS, Hawash AA, Voss AA, and Rich MM, 2019. Treatment of myotonia congenita with retigabine in mice. Exp Neurol 315, 52–59. [PubMed: 30738808]

Dupont C, Novak K, Denman K, Myers JH, Sullivan JM, Walker PV 2nd, Brown NL, Ladle DR, Bogdanik L, Lutz CM, A AV, Sumner CJ, and Rich MM, 2020. TRPV4 Antagonism Prevents Mechanically Induced Myotonia. Ann Neurol.

Fraser JA, Huang CL, and Pedersen TH, 2011. Relationships between resting conductances, excitability, and t-system ionic homeostasis in skeletal muscle. J Gen Physiol 138, 95–116. [PubMed: 21670205]

Hawash AA, Voss AA, and Rich MM, 2017. Inhibiting persistent inward sodium currents prevents myotonia. Ann Neurol 82, 385–395. [PubMed: 28833464]

Koch MC, Steinmeyer K, Lorenz C, Ricker K, Wolf F, Otto M, Zoll B, Lehmann-Horn F, Grzeschik KH, and Jentsch TJ, 1992. The skeletal muscle chloride channel in dominant and recessive human myotonia. Science 257, 797–800. [PubMed: 1379744]

Lamb GD, and Stephenson DG, 2018. Measurement of force and calcium release using mechanically skinned fibers from mammalian skeletal muscle. J Appl Physiol (1985) 125, 1105–1127. [PubMed: 30024333]

Lehmann-Horn F, Jurkat-Rott K, and Rudel R, 2008. Diagnostics and therapy of muscle channelopathies--Guidelines of the Ulm Muscle Centre. Acta Myol 27, 98–113. [PubMed: 19472919]

Lo Monaco M, D'Amico A, Luigetti M, Desaphy JF, and Modoni A, 2015. Effect of mexiletine on transitory depression of compound motor action potential in recessive myotonia congenita. Clin Neurophysiol 126, 399–403. [PubMed: 25065301]

Lossin C, and George AL Jr., 2008. Myotonia congenita. Adv Genet 63, 25–55. [PubMed: 19185184]

Matthews E, and Hanna MG, 2014. Repurposing of sodium channel antagonists as potential new anti-myotonic drugs. Exp Neurol 261, 812–815. [PubMed: 25218042]

Metzger S, Dupont C, Voss AA, and Rich MM, 2020. Central Role of Subthreshold Currents in Myotonia. Ann Neurol 87, 175–183. [PubMed: 31725924]

Myers JH, Denman K, DuPont C, Hawash AA, Novak KR, Koesters A, Grabner M, Dayal A, Voss AA, and Rich MM, 2021. The mechanism underlying transient weakness in myotonia congenita. Elife 10.

Novak KR, Norman J, Mitchell JR, Pinter MJ, and Rich MM, 2015. Sodium channel slow inactivation as a therapeutic target for myotonia congenita. Ann Neurol 77, 320–332. [PubMed: 25515836]

Palade PT, and Barchi RL, 1977. Characteristics of the chloride conductance in muscle fibers of the rat diaphragm. J Gen Physiol 69, 325–342. [PubMed: 15046]

Palade PT, and Barchi RL, 1977. On the inhibition of muscle membrane chloride conductance by aromatic carboxylic acids. J Gen Physiol 69, 879–896. [PubMed: 894246]

Ricker K, Haass A, Hertel G, and Mertens HG, 1978. Transient muscular weakness in severe recessive myotonia congenita. Improvement of isometric muscle force by drugs relieving myotomic stiffness. J Neurol 218, 253–262. [PubMed: 81274]

Robin G, and Allard B, 2013. Major contribution of sarcoplasmic reticulum Ca(2+) depletion during long-lasting activation of skeletal muscle. J Gen Physiol 141, 557–565. [PubMed: 23630339]

Sanders DB, 1976. Myotonia congenita with painful muscle contractions. Arch Neurol 33, 580–582. [PubMed: 942314]

Schneider MF, and Simon BJ, 1988. Inactivation of calcium release from the sarcoplasmic reticulum in frog skeletal muscle. J Physiol 405, 727–745. [PubMed: 2855645]

Shang W, Lu F, Sun T, Xu J, Li LL, Wang Y, Wang G, Chen L, Wang X, Cannell MB, Wang SQ, and Cheng H, 2014. Imaging Ca2+ nanosparks in heart with a new targeted biosensor. Circ Res 114, 412–420. [PubMed: 24257462]

Simon BJ, Klein MG, and Schneider MF, 1991. Calcium dependence of inactivation of calcium release from the sarcoplasmic reticulum in skeletal muscle fibers. J Gen Physiol 97, 437–471. [PubMed: 2037837]

Statland JM, Bundy BN, Wang Y, Rayan DR, Trivedi JR, Sansone VA, Salajegheh MK, Venance SL, Ciafaloni E, Matthews E, Meola G, Herbelin L, Griggs RC, Barohn RJ, and Hanna MG, 2012. Mexiletine for symptoms and signs of myotonia in nondystrophic myotonia: a randomized controlled trial. Jama 308, 1357–1365. [PubMed: 23032552]

Steinmeyer K, Klocke R, Ortland C, Gronemeier M, Jockusch H, Grunder S, and Jentsch TJ, 1991. Inactivation of muscle chloride channel by transposon insertion in myotonic mice. Nature 354, 304–308. [PubMed: 1659665]

Stohr M, Schlote W, Bundschu HD, and Reichenmiller HE, 1975. [Myopathia myotonica. A new type of hereditary muscle disease (author's transl)]. J Neurol 210, 41–66. [PubMed: 51068]

Trivedi JR, Cannon SC, and Griggs RC, 2014. Nondystrophic myotonia: challenges and future directions. Exp Neurol 253, 28–30. [PubMed: 24361411]

Wallinga W, Meijer SL, Alberink MJ, Vliek M, Wienk ED, and Ypey DL, 1999. Modelling action potentials and membrane currents of mammalian skeletal muscle fibres in coherence with potassium concentration changes in the T-tubular system. Eur Biophys J 28, 317–329. [PubMed: 10394624]

Wang X, Nawaz M, DuPont C, Myers JH, Burke SR, Bannister RA, Foy BD, Voss AA, and Rich MM, 2022. The role of action potential changes in depolarization-induced failure of excitation contraction coupling in mouse skeletal muscle. Elife 11.

Wang ZM, Messi ML, and Delbono O, 1999. Patch-clamp recording of charge movement, Ca2+ current, and Ca2+ transients in adult skeletal muscle fibers. Biophys J 77, 2709–2716. [PubMed: 10545370]

Zot AS, and Potter JD, 1987. The effect of [Mg2+] on the Ca2+ dependence of ATPase and tension development of fast skeletal muscle. The role of the Ca2+-specific sites of troponin C. J Biol Chem 262, 1966–1969. [PubMed: 2950083]

Highlights:

- Myotonic muscle develops seconds to minutes long plateau potentials to near −35 mV
- Intracellular calcium remains elevated during the early phase of plateau potentials
- Elevation of calcium causes contraction of electrically inexcitable muscle
- During prolonged plateau potentials, myotonia transitions to flaccid paralysis

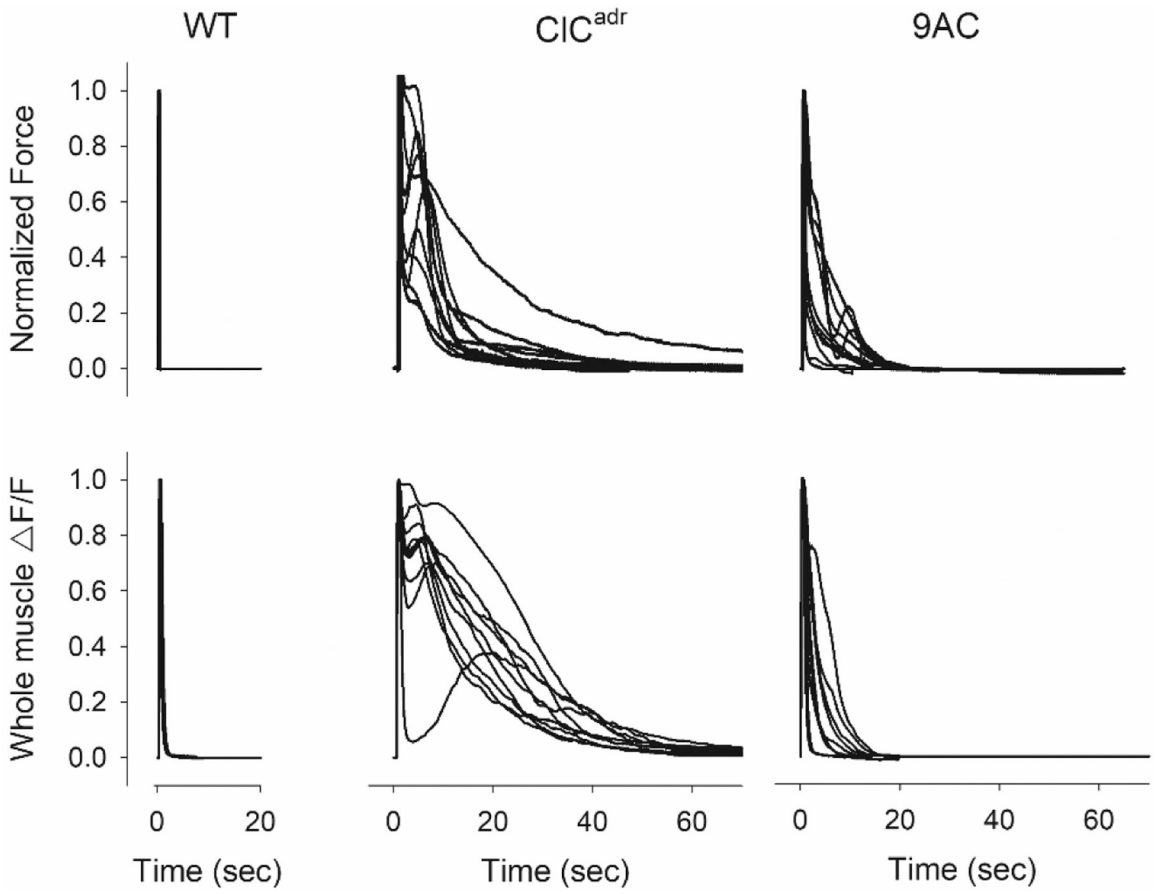

Fig 1.

EDL whole muscle tetanic force for wild type (WT) muscle as well as the two models of myotonia congenita. Muscle was stimulated in all traces for 0.4 s at 100 Hz. Shown on the top left are superimposed force traces from 4 wild type muscles. In the top middle are the force traces from 10 ClC^{adr} muscles and on the top right are traces from 11 9AC treated muscles. In both models of myotonia congenita contraction lasting longer than 0.4 s, representing myotonia, was present. Each force trace was normalized to the peak force at the end of at 100 Hz stimulation. On the bottom row are the whole muscle Ca^{2+} signals from a different set of muscles. 10 wild type muscles, 10 ClC^{adr} muscles and 10 9AC treated muscles were imaged. Each Ca^{2+} trace was normalized to the peak at the end of 100 Hz stimulation.

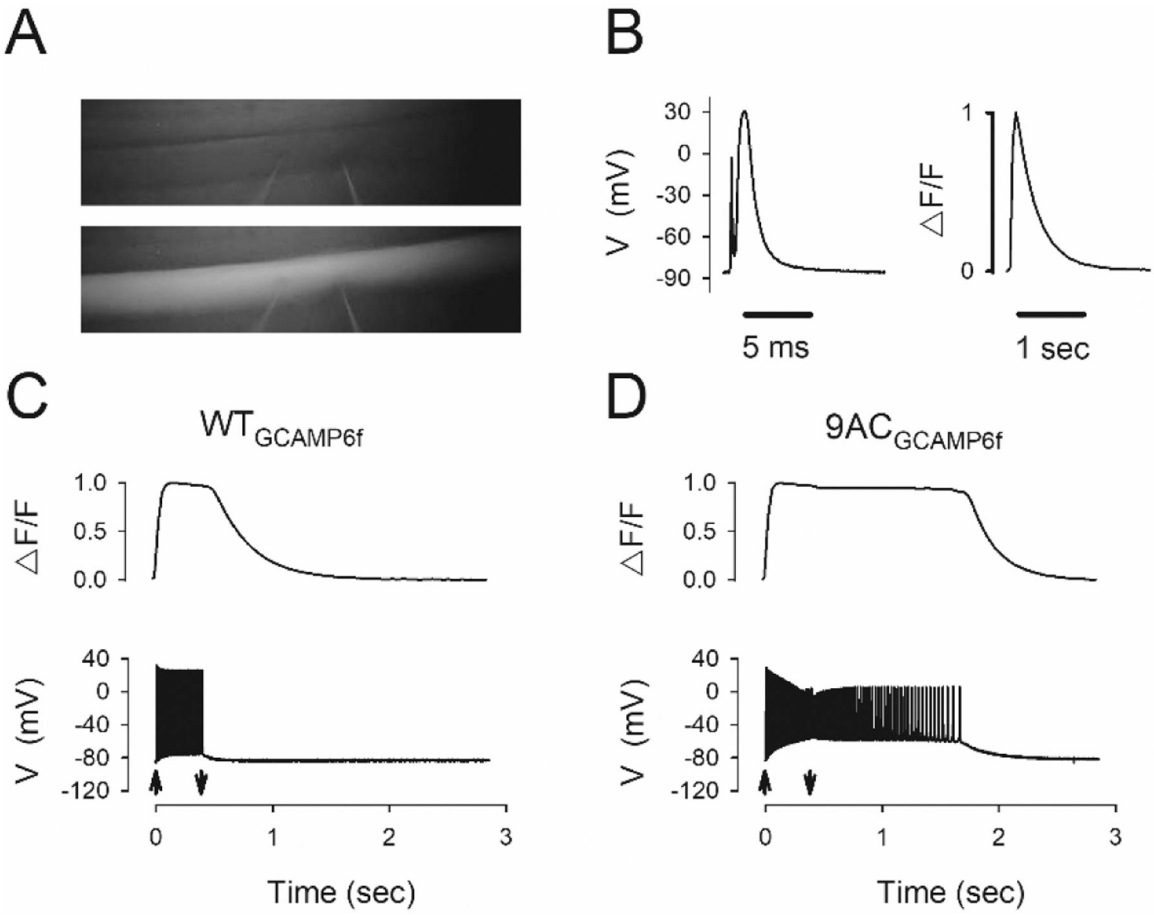

Fig 2-

Simultaneous intracellular recording of membrane potential and imaging of Ca^{2+} in individual muscle fibers expressing GCAMP6f. A) The top image is of a fiber at rest. The bottom image shows the fiber after triggering of a single action potential. The electrodes can faintly be seen impaling the fiber at the center of the image. B) An action potential and ΔF/F for a fiber following a single action potential. In the voltage trace there is a stimulus artifact prior to initiation of the action potential. C) ΔF/F and the intracellular voltage from a fiber during stimulation at 100 Hz for 0.4 s. D) ΔF/F and the intracellular voltage for a 9AC treated fiber. There is a myotonic discharge lasting 1.2s following termination of stimulation. Ca^{2+} remained elevated during the myotonic discharge and decayed to baseline following termination of the discharge. In C and D the up arrow represents the beginning of 100 Hz stimulation and the down arrow represents its termination.

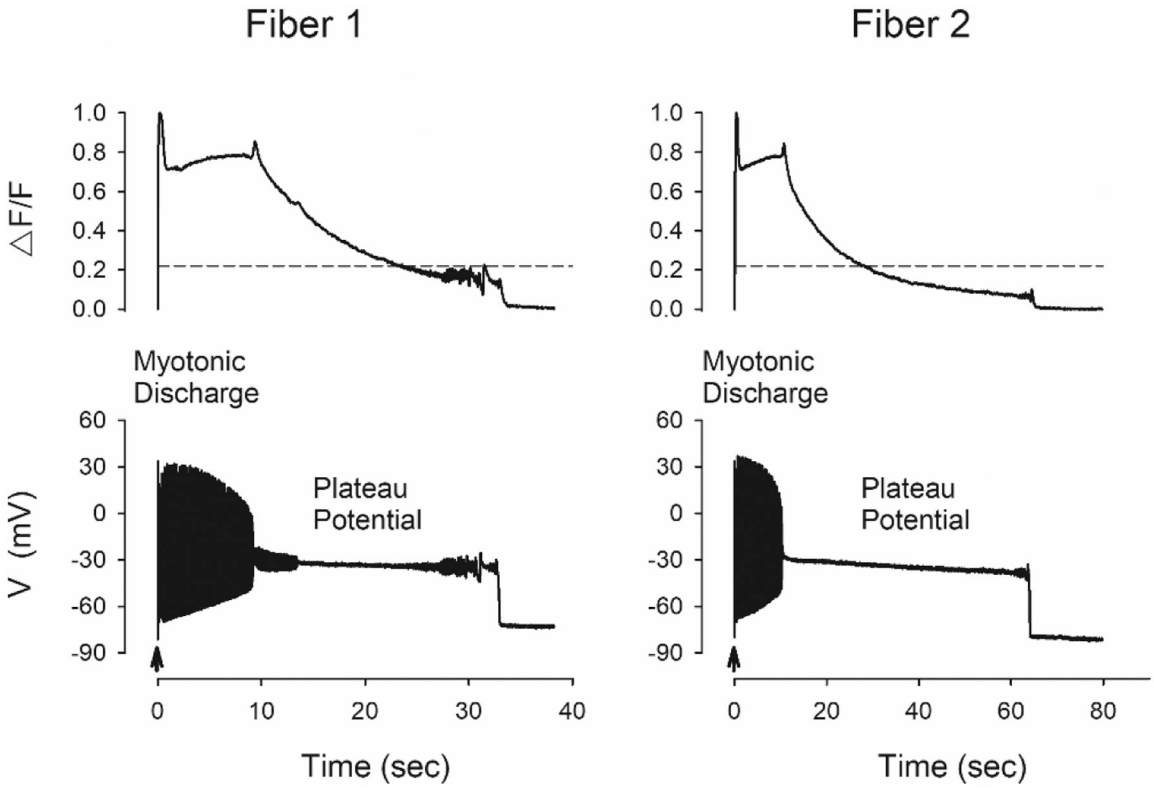

Fig 3-

Simultaneous intracellular recording and Ca^{2+} imaging in 2 $ClC^{adr}_{GCAMP6f}$ fibers. The horizontal dotted line in each Ca^{2+} trace represents the ΔF/F triggered by a single action potential in the same fiber. The up arrow in each voltage traces represents the period of 100 Hz stimulation. The time base is too compressed to also show the down arrow representing the termination of stimulation as was done in Figure 2.

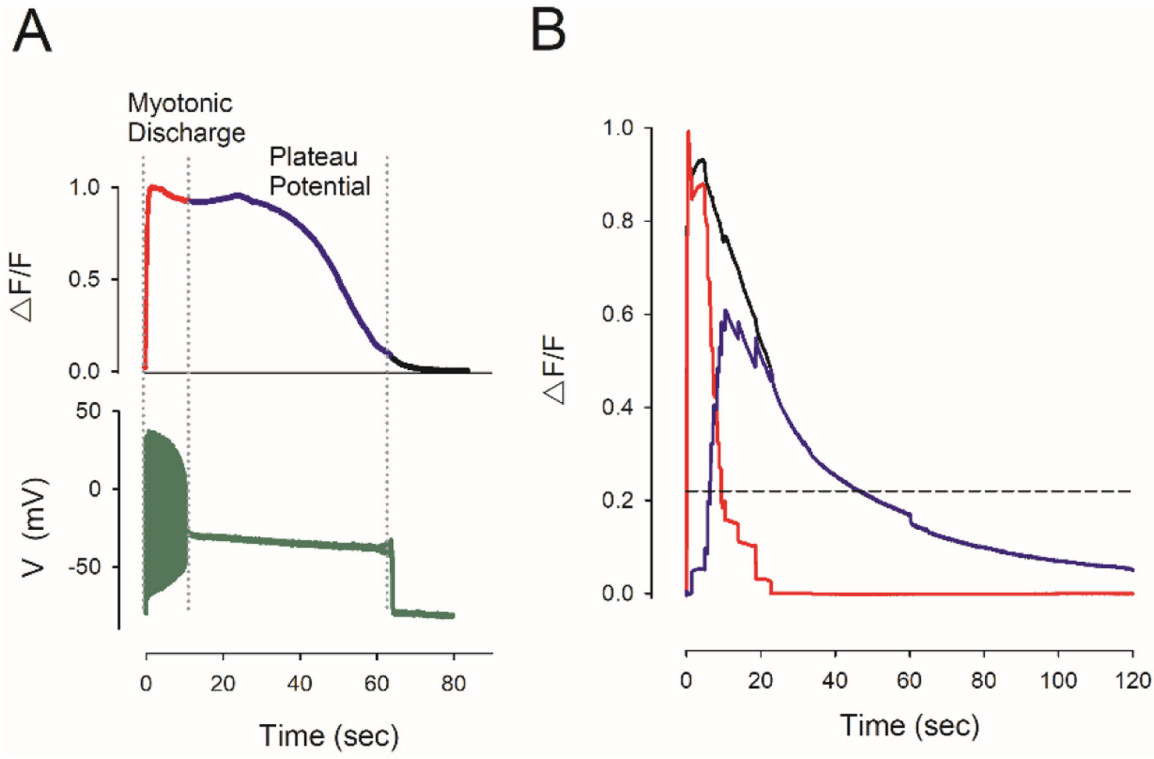

Fig 4-

Elevation of ΔF/F due to myotonic discharges and plateau potentials. A) Classification of elevation of ΔF/F as occurring during myotonic discharges versus a plateau potential in a $ClC^{adr}_{GCAMP6f}$ fiber. B) Plot of the ΔF/F from 20 $ClC^{adr}_{GCAMP6f}$ fibers normalized to the ΔF/F immediately following termination of 0.4 s of 100 Hz stimulation. The black trace is the average ΔF/F trace. The red trace is the elevation of ΔF/F occurring during myotonic discharges and the blue trace is the elevation of ΔF/F during plateau potentials. For reference, the average ΔF/F triggered by a single action potential is plotted as a horizontal dotted line.

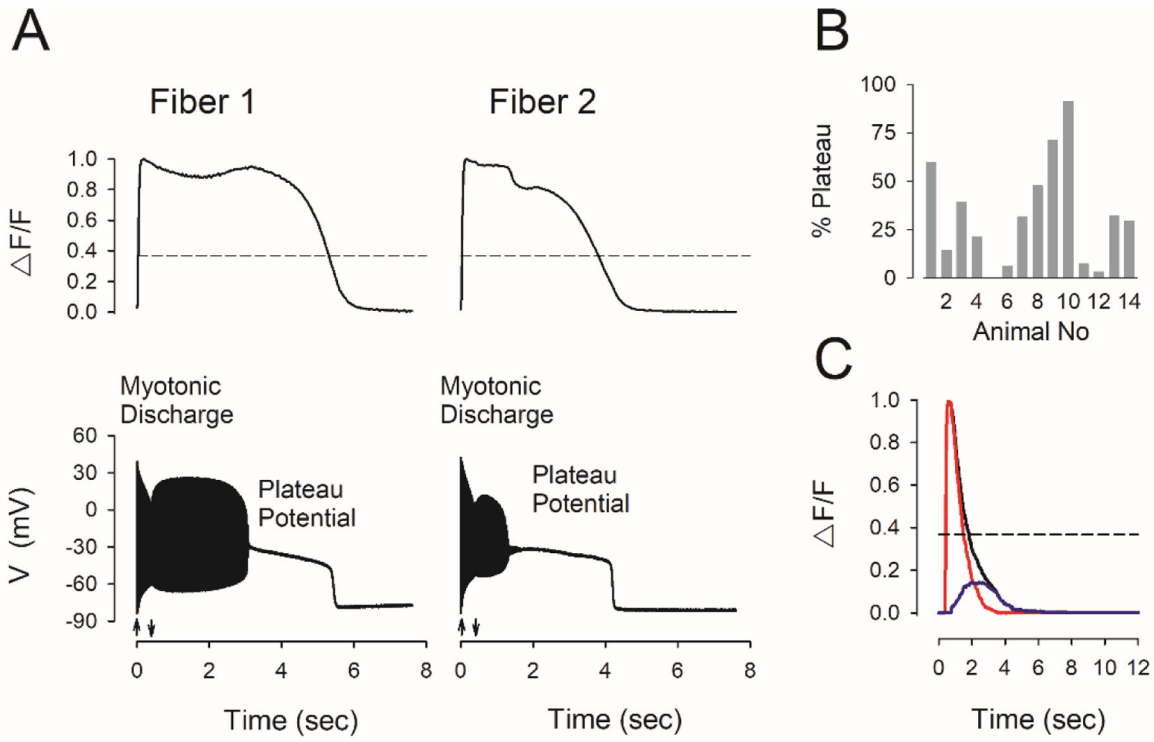

Figure 5.

Elevation of ΔF/F due to myotonic discharges and plateau potentials in $9AC_{GCAMP6f}$ fibers. A) Simultaneous intracellular recording and imaging of Ca^{2+} in 2 $9AC_{GCAMP6f}$ fibers. The horizontal dotted line in each Ca^{2+} trace represents the ΔF/F triggered by a single action potential. The up arrow in each voltage traces represents the initiation of 100 Hz stimulation and the down arrow its termination. B) Plot of the percentage of fibers with plateau potentials from 14 muscles treated with 9AC. C) Plot of the mean ΔF/F immediately following termination of 0.4 s of Hz stimulation from 372 fibers. The black trace is the average ΔF/F trace. The red trace is the elevation of ΔF/F occurring during myotonic discharges and the blue trace is the elevation of ΔF/F during plateau potentials. For reference, a horizontal dotted line representing the average ΔF/F triggered by a single action potential is plotted.

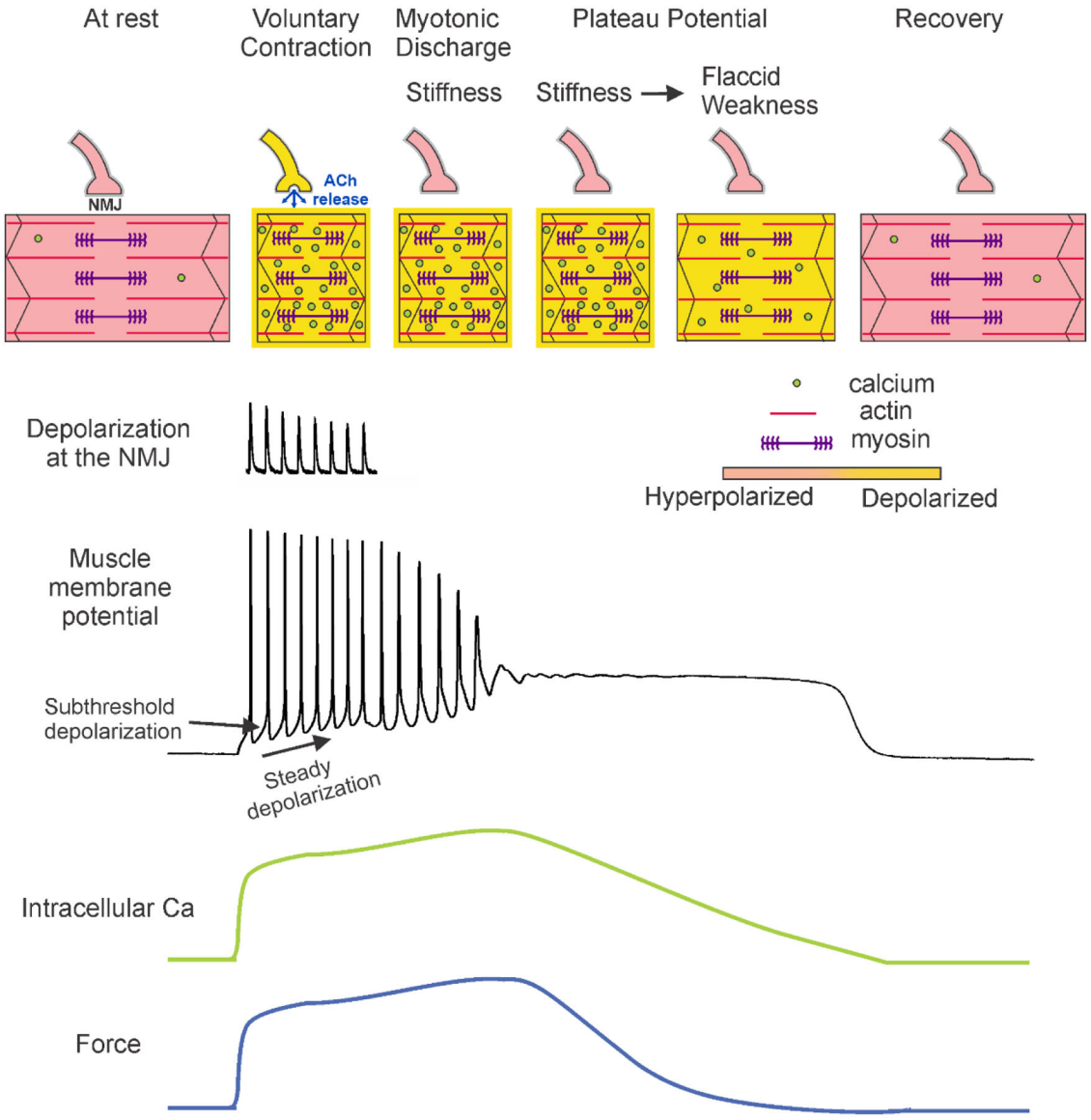

Fig 6:

Voluntary contraction in myotonia congenita triggers progression through states of hyper- and hypo-excitability. Sustained voluntary contraction of skeletal muscle is initiated at the neuromuscular junction by repeated endplate potentials, which trigger repeated firing of muscle action potentials. With repetitive firing, there is build-up of steady depolarization, which combines with subthreshold depolarization to trigger a myotonic discharge following cessation of stimulation by the neuromuscular junction. Throughout voluntary movement and the myotonic discharge, Ca^{2+} remains elevated such that force is generated. When myotonic discharges transition into plateau potentials, Ca^{2+} is initially elevated, which prolongs myotonia. During prolonged plateau potentials, intracellular Ca^{2+} decreases such that myotonia decreases and muscle transitions from stiffness to flaccid paralysis. Finally, there is sudden repolarization from the plateau potential to the normal resting potential,

which is accompanied by the return to normal excitability. NMJ = neuromuscular junction, ACh = acetylcholine.